

# Development of Nondestructive Imaging Analysis Method Using Muonic X-ray with a Double-Sided Silicon Strip Detector

I-Huan Chiu, Kazuhiko Ninomiya, Shin'ichiro Takeda, Meito Kajino, Miho Katsuragawa, Shunsaku Nagasawa, Atsushi Shinohara, Tadayuki Takahashi, Ryota Tomaru, Shin Watanabe, Goro Yabu

**Abstract**—In recent years, a nondestructive elemental analysis method based on muonic X-ray measurements has been developed and applied for various samples. Muonic X-rays are emitted after the formation of a muonic atom, which occurs when a negatively charged muon is captured in a muon atomic orbit around the nucleus. Because muonic X-rays have a higher energy than electronic X-rays due to the muon mass, they can be measured without being absorbed by a material. Thus, estimating the two-dimensional (2D) elemental distribution of a sample became possible using an X-ray imaging detector. In this work, we report a non-destructive imaging experiment using muonic X-rays at Japan Proton Accelerator Research Complex. The irradiated target consisted of a polypropylene material, and a double-sided silicon strip detector, which was developed as an imaging detector for astronomical observation, was employed. A peak corresponding to muonic X-rays from the carbon atoms in the target was clearly observed in the energy spectrum at an energy of 14 keV, and 2D visualizations were successfully reconstructed to reveal the projection image from the target. This result demonstrates the potential of the nondestructive elemental imaging method that is based on muonic X-ray measurement. To obtain a higher position resolution for imaging a smaller target, a new detector system will be developed to improve the statistical analysis in further research.

**Keywords**—DSSD, Muon, Muonic X-ray, Imaging, Non-destructive analysis

## I. INTRODUCTION

**E**LEMENTAL analysis methods, such as X-ray fluorescence and mass spectrometry, are among the most fundamental techniques in natural sciences and are used to analyze the structure of materials. A nondestructive elemental analysis method is particularly suitable for precious samples. Methods using muonic atoms offer a huge potential for nondestructive elemental analysis. A muonic atom is formed when a negative muon is captured in the muon atomic orbit, and characteristic muonic X-rays are emitted from the muonic atom during the transition of the muon to the ground state. Because the mass of the muon is approximately 207 times that of the electron, the energy of muonic X-rays is much higher than

that of electronic X-rays. These hard X-rays can pass through a material without being absorbed. Therefore, nondestructive elemental analysis can be performed using muonic X-rays for any element, including light ones for bulk materials. Recently, this method has been applied to conduct elemental analyses in various research fields, such as archaeology and astronomy. To demonstrate the possibility of analyzing the elemental components of a sample using muonic X-rays, Terada et al. quantified the elemental component contribution of meteorites via muon beam analysis [1], [2]. Takaura et al. proposed a nondestructive analysis method for medical inheritances, and successfully detected medication contents in glass bottles [3]. Moreover, since the muon stopping depth in a sample can be controlled by changing the energy of the incident muon beam, an elemental depth-profiling analysis method was developed for Japanese gold coins [4] and Roman coins [5]. Thus, the nondestructive elemental analysis method using muonic X-rays has been widely adopted in the last decade. This method can also provide isotopic information. Kudo et al. determined the variations in isotopic abundance of lead plate samples using the isotope shift of muonic X-rays [6]. To further develop this technique, a two-dimensional (2D) elemental distribution measurement would be highly beneficial. To obtain the 2D image of a sample using muonic X-rays, a hard X-ray imaging detector with high resolution and low noise was developed for astronomical observation in the 10- to 100-keV range by Takeda et al. [7]. In this work, we report a nondestructive 2D imaging technique for a spherical-shape target using muonic X-rays with a double-sided silicon strip detector (DSSD).

## II. DOUBLE-SIDED SILICON STRIP DETECTOR

The DSSD technology, which provides a large sensitivity area with high energy resolution and low noise [8], was developed as a position-sensitive detection technique for astronomical observations to measure both hard and soft X-rays. In this study, the DSSD that was employed in the new Japanese X-ray Astronomy Satellite [9], which is characterized by an imaging area of  $32 \times 32 \text{ mm}^2$  and a thickness of  $500 \mu\text{m}$ , was used to obtain the 2D spatial information of muonic X-rays. Figure 1 shows the basic geometry of this DSSD including the orthogonal configuration of the electrode system. Each side on the surface of the silicon sensor has 128 strips, which were p+ and n+ implanted for the cathode and

I. Chiu and K. Ninomiya are with the Radioisotope Research Center Institute Radiation Sciences Osaka University, 1-1 Yamadaoka, Suita, Osaka, 565-0871, Japan (e-mail: ichiu@rirc.osaka-u.ac.jp)

M. Kajino and A. Shinohara are with the Graduate School of Science, Osaka University, 1-1, Machikaneyama, Toyonaka, Osaka, 560-0043, Japan

S. Takeda, M. Katsuragawa, R. Tomaru, G. Yabu, S. Nagasawa, and T. Takahashi are with the Kavli Institute for the Physics and Mathematics of the Universe (WPI), University of Tokyo, 5-1-5 Kashiwanoha, Kashiwa, Chiba 277-8583, Japan

S. Watanabe is with the Institute of Space and Astronautical Science, Japan Aerospace Exploration Agency (ISAS/JAXA), 3-1-1 Yoshinodai, Chuo-ku, Sagami-hara, Kanagawa 252-5210, Japan

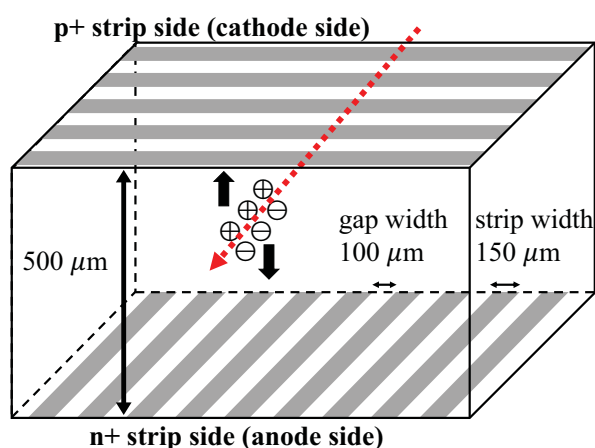


Fig. 1. Schematic of the DSSD with a thickness of 500  $\mu\text{m}$ . The anode and cathode electrodes are on the p-side and n-side, respectively. The gray bands on both sides show the orthogonal structure of the anode and cathode electrodes, which are composed of strips with a pitch of 250  $\mu\text{m}$ . The orthogonal structure provides a way to measure the 2D coordinates of incident photons. The DSSD offers the capability of imaging with a large sensitive area of 32  $\times$  32  $\text{mm}^2$ . The operation voltage was kept constant at 200 V.

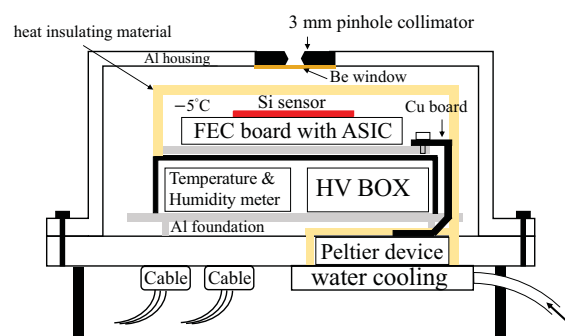


Fig. 2. Cutaway view of the Al housing for the DSSD. A pinhole collimator with a diameter of 3 mm was placed at the top of the Al housing to directly acquire the muonic X-ray image. The geometry of the pinhole collimator provides an FOV of 50°. The heat-insulating material utilized to isolate the silicon sensor from surrounding warm air is indicated by the thick yellow line. The FEC board is cooled down by a Cu board, which is connected to the cold side of the Peltier device. The temperature of the FEC board was kept at  $-5^\circ\text{C}$  during operation.

anode sides, respectively. The strip width and gap width are 150 and 100  $\mu\text{m}$ , respectively. When hard and soft X-rays release their energy onto the silicon sensor, a considerable number of electron-hole pairs are generated depending on their energy loss. These electron-hole pairs are then collected by the anode and cathode electrodes on the two sides of the DSSD to estimate the energy deposition. The intensity of the charge signal obtained from each electrode is converted into a digital pulse height after subtracting the common mode noise [10], and the signals are amplified via a dedicated analog application-specific integrated circuit, which has a low-noise performance [11]. For normal DSSD operating conditions, the applied bias voltage is set to 200 V; this value depends on the DSSD thickness and the strip gap [12]. As the readout noise caused by the leakage current on the DSSD is highly related to the temperature [8], a low-temperature operation provides

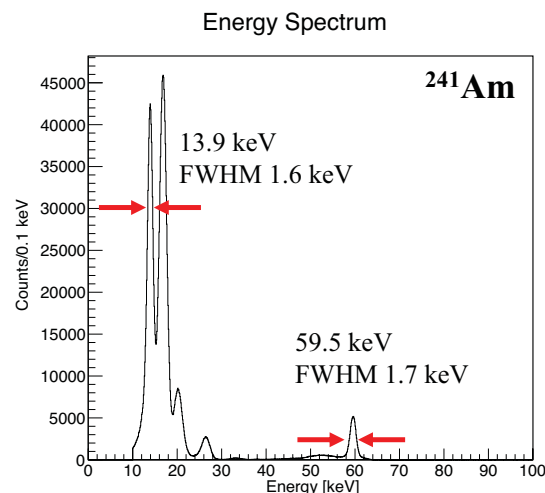


Fig. 3. Energy spectrum of the 128 strips on the p-side using  $^{241}\text{Am}$ . The energy resolution (FWHM) of the DSSD was investigated on the basis of the Gaussian function. FWHM values of 1.6 and 1.7 keV were obtained at 13.9 and 59.5 keV, respectively.

a higher energy resolution. The performance of the DSSD has been investigated using an  $^{241}\text{Am}$  radioactive source. An energy resolution (described in terms of the full width at half maximum (FWHM)) of 0.9 keV at 13.9 keV was obtained at a temperature of  $-20^\circ\text{C}$  by Sato et al. [9], whereas an FWHM of 1.5 keV at 59.5 keV was achieved at a temperature of  $-10^\circ\text{C}$  [7]. In addition, the orthogonal configuration of the electrode system on the two sides of the DSSD is capable to provide information on the 2D position of an incident photon. Therefore, thanks to the fine strip pitch, a high spatial resolution of a few hundred micrometers was obtained for the 2D position.

For the muon-irradiation experiment, the DSSD was placed inside an Al housing, as shown in Figure 2. To measure the projection image from the target using muonic X-rays, the DSSD was combined with a W pinhole collimator with a diameter of 3 mm and a thickness of 8 mm. This collimator was placed at the top of the housing above the Be window, and a field of view of 50° was obtained. As shown in the sketch of the housing, the Cu board that connects the cold side of the Peltier device to the front end card (FEC) board of the readout system of the DSSD was designed for cooling the FEC board. Hence, the DSSD could be operated at a temperature of  $-5^\circ\text{C}$  to reduce the noise associated with the leakage current of the detector. To keep the temperature of the FEC board at  $-5^\circ\text{C}$  during the muon experiment, a heat-insulating material (the thick yellow line in Figure 2) was used to isolate the silicon sensor from the surrounding warm air. Moreover, water cooling was utilized for removing heat from the hot side of the Peltier device. Temperature and humidity meters were placed beside the bias voltage control box (HV BOX) in the housing to monitor the status of the Al housing during operation.

Figure 3 presents the spectrum of the 128 strips on the p-side of the detector using the  $^{241}\text{Am}$  source. An FWHM of 1.7 keV at 59.5 keV, corresponding to an energy resolution of  $\Delta E/E = 2.9\%$ , was achieved. In the low-energy region,

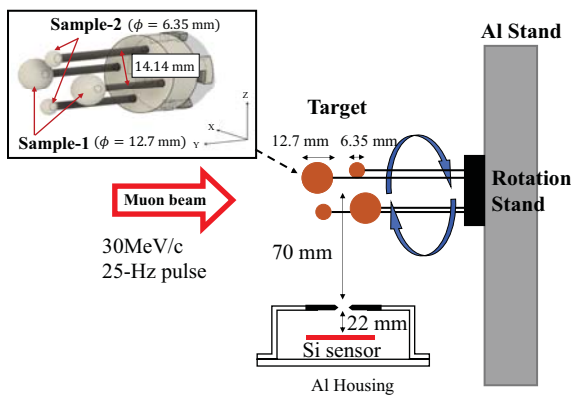


Fig. 4. Experiment setup of the MUSE/J-PARC D2 beam line. The irradiated samples with diameters of 12.7 and 6.35 mm were fixed onto the Al stand using Al rods. The 12.7-mm sample is here referred to as “Sample-1”, whereas the 6.35-mm sample is referred to as “Sample-2”. The samples, which were placed at the downstream of the muon beam, were spun along the muon beam axis during the muon irradiation process to obtain the projection images. The distances from the pinhole collimator to the sample and from the pinhole collimator to the silicon sensor were 70 and 22 mm, respectively.

the DSSD provides an energy resolution of 11.3% with an FWHM of 1.6 keV at 13.9 keV. By comparing these results with the energy resolution of 0.9 keV at 13.9 keV reported in a previous study [9], the effect of the temperature on the energy spectrum was confirmed. At a temperature of  $-5^{\circ}\text{C}$ , the huge noise component due to the leakage current of the detector degrades the performance of the DSSD. Although the noise level of the energy spectrum needs to be improved for the current detector system, it was ensured that the DSSD spatial resolution was sufficiently high for the muonic X-ray imaging experiment.

### III. EXPERIMENT

To ensure a high intensity for the muon beam for the statistical analysis with muonic X-rays, the muon experiment was conducted at the MUon Science Establishment (MUSE) at the Japan Proton Accelerator Research Complex (J-PARC), which provides the world’s most intense pulsed negative muon beam [13]. At J-PARC, the proton beam is accelerated to an energy of 3 GeV with 25-Hz beam cycles and collides with a muon-production target. By tuning the beam transportation magnet system of the D2 beam line at MUSE, the momentum of the muon beam was tuned to be 30 MeV/c based on the quality of the observed images of the DSSD. As sketched in Figure 4, the samples, which consist of four spherical-shaped polypropylene ( $(\text{C}_3\text{H}_6)_n$ ) balls, were fixed to the rotation stand using Al rods and installed at the downstream of the muon beam for muon irradiation. The samples with diameters of 12.7 and 6.35 mm are referred to as “Sample-1” and “Sample-2”, respectively. On the basis of Monte Carlo simulations using the Geant4 toolkit [14], over 95% of input muons with a momentum of 30 MeV/c were stopped at a distance in the range of 0.93–1.39 mm from the surface of the polypropylene material. When the samples were exposed to the muon beam in air, the DSSD was placed below the samples to measure the muonic X-ray signals originating from

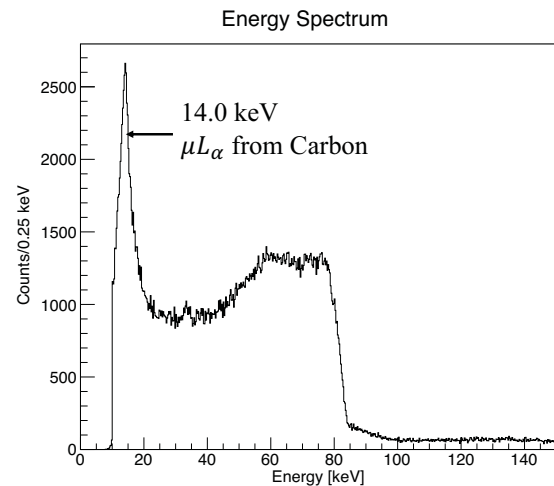


Fig. 5. Energy spectrum obtained from the DSSD. A clear peak was identified as  $\mu\text{C-L}\alpha$  from samples with an energy of 14.0 keV. The large amount of data in the energy range of 60–80 keV is because the background was dominated by  $\mu\text{Al-L}\alpha$  with an energy of 66.1 keV. The continuum component in the energy spectrum originates from the Compton effect and bremsstrahlung emission.

the samples. The distances from the pinhole collimator to the sample and from the pinhole collimator to the silicon sensor were 70 and 22 mm, respectively. To validate the images collected by the DSSD, the samples were spun along the muon beam axis using a rotation stand to obtain the rotation projection images. The projection images were acquired at four specified rotation angles, namely,  $0^{\circ}$ ,  $90^{\circ}$ ,  $180^{\circ}$ , and  $270^{\circ}$ . The muon irradiation at each angle lasted approximately 2 h.

## IV. RESULTS AND DISCUSSION

### A. Spectral analysis

Figure 5 shows the energy spectrum observed on the p-side of the DSSD during muon irradiation. The sources of the energy distribution were investigated on the basis of the muonic X-ray signal from the samples and other possible backgrounds. Because of the chemical formula of the polypropylene balls, the signal from the samples was considered to be that of the muonic X-rays for hydrogen and carbon ( $\mu\text{H}$  and  $\mu\text{C}$ ). However,  $\mu\text{H}$  with an energy of approximately 2 keV exceeds the detectable energy range of the DSSD in air, so  $\mu\text{C}$  was the only signal that could be measured from the samples in this experiment.  $\mu\text{C-K}\alpha$  with an energy of 75 keV [15] represented the muonic X-rays with the highest intensity from carbon. However, the silicon sensor with a thickness of 500  $\mu\text{m}$  was unable to provide a sufficient photoabsorption efficiency for these high-energy photons. These muonic X-rays with high energy passed through the DSSD without the detector being able to capture their total energy. Therefore,  $\mu\text{C-L}\alpha$  with an energy of 14.0 keV [16] was expected to be the main signal from the DSSD for this experiment. A clear peak in the Gaussian distribution with a mean value of  $14.0 \pm 0.02$  keV was observed in the energy spectrum. Owing to the good agreement between the measured mean peak value and the corresponding theoretical value, the peak was identified as the  $\mu\text{C-L}\alpha$  signal. In order to select the signals from the  $\mu\text{C-L}\alpha$

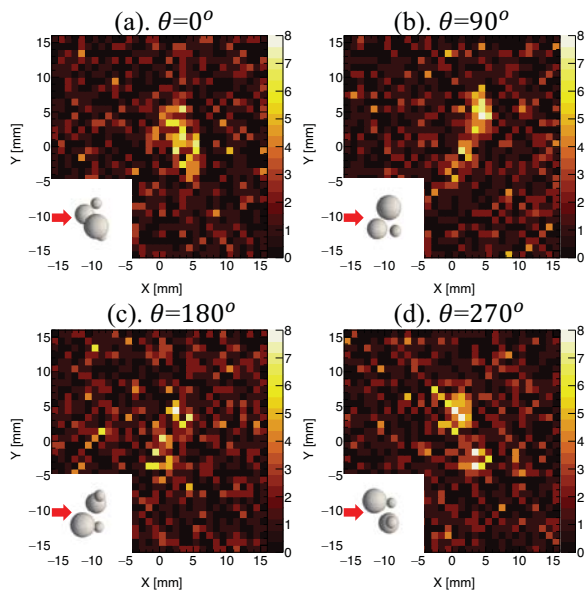


Fig. 6. Reconstructed images using the  $\mu C-L_{\alpha}$  line in the energy band from 12 to 18 keV. (a)–(d) Images of the target at the rotation angles of  $0^{\circ}$ ,  $90^{\circ}$ ,  $180^{\circ}$ , and  $270^{\circ}$ , respectively. The actual distribution of the target with the muon beam (red arrow) is displayed in the left bottom corner of each panel. In a set comprising these four images, the projections reveal the spherical shape of Sample-1, and the rotation motion during muon irradiation is also observed.

line, the events in the energy band from 12 to 18 keV were used for image reconstruction. Besides the  $\mu C$  signal from the samples, the muonic X-rays from Al ( $\mu Al-L_{\alpha}$ ) with an energy of 66.1 keV were considered to be a possible background source. Because a number of muons passed through the sample and stopped at the Al stand,  $\mu Al-L_{\alpha}$ , which penetrated the Al housing due to their high energy, constituted a background source. As shown in Figure 5, the energy spectrum displays a large amount of data in the range of 60–80 keV due to the contribution of  $\mu Al-L_{\alpha}$ . This pronounced background from the Al stand was also confirmed by the Monte Carlo simulation. The contribution of  $\mu Al-L_{\alpha}$  is a serious problem in the energy spectrum and image reconstruction. In addition, the continuum component in the entire energy spectrum is due to the Compton effect and bremsstrahlung emission.

### B. Image reconstruction

Thanks to the orthogonal structure of the DSSD electrodes, the 2D coordinate information of an incident photon can be obtained. The location of an incident photon on the x- and y-axis was identified on the basis of the center positions of the strips on the p-side and n-side of the DSSD, respectively. The image from the sample was reconstructed using the events in the energy band from 12 to 18 keV, corresponding to the  $\mu C-L_{\alpha}$  line. Figure 6(a)–(d) presents the image from the irradiated target at four rotation angles, and the actual distribution is shown in the left bottom corner of each panel. Because the muons were captured on the surface of the samples, the projection image on the DSSD should be close to a half circle rather than a spherical shape. Moreover, the enlargement effect

due to the pinhole collimator needs to be taken into account. The image on the DSSD was enlarged from its actual size by the scale factor (SF) described in the following formula:

$$SF = d_1/d_2, \quad (1)$$

where  $d_1 = 22$  mm is the distance from the silicon sensor to the pinhole collimator, and  $d_2 = 70$  mm is the distance from the pinhole collimator to the sample. Thus, the size of the projection images rendered onto the DSSD from Sample-1 can be computed taking into account the collimator effect. In conclusion, the projection from Sample-1 on the DSSD should yield two half circles with a radius of 2 mm. Furthermore, the spatial resolution of the pinhole collimator was analyzed according to the definition from Brownell [17]:

$$\text{Resolution} = \left(1 + \frac{d_1}{d_2}\right) \times r, \quad (2)$$

where  $r = 3$  mm is the diameter of the pinhole collimator. On the basis of this equation, the spatial resolution of the image was estimated to be 5.03 mm.

In Figure 6, the set of images reveal two half-circle projections from Sample-1, and the rotational motion is clearly observed. The size of the reconstructed image was calculated from Figure 6(b), because the other plots did not provide a sufficiently high amount of data for quantitative comparison. The signal distributions in Figure 6(b) along the x- and y-axis were smoothed using Gaussian functions with FWHM values of 2.94 and 5.75 mm, respectively. By comparing the FWHM of 2.94 (5.75) mm with the expected size of 2 (4) mm for the x (y)-axis, the obtained difference of 0.94 (1.75) mm is much smaller than the spatial resolution of 5.03 mm. Thus, because the reconstructed image does not show any significant discrepancy with respect to the expected shape of the projection image, the good imaging capability of the DSSD was confirmed. To sum up, the projection images of Sample-1 were successfully measured by the DSSD using muonic X-rays.

Unlike the projection images of Sample-1, the boundaries of the images of Sample-2 still need to be improved. Because the total cross-sectional area of Sample-2 with a diameter of 6.35 mm is four times smaller than that of Sample-1, the amount of data was too small to distinguish the signal from the  $\mu Al-L_{\alpha}$  background. To improve the imaging performance of the DSSD for a smaller sample, an advanced configuration for the detector system should be developed to decrease the possible noise and background.

## V. CONCLUSIONS

Nondestructive elemental analysis methods with muonic X-rays have been utilized in various fields to successfully quantify the elemental composition of samples. In this work, a method of perform nondestructive elemental analysis combined with imaging using the high-sensitivity DSSD is proposed. The experiment was implemented on the D2 beam line at MUSE/J-PARC, which provides a high-intensity negative muon beam. The detector system, which consists of a DSSD, pinhole collimator, and an Al housing, was utilized to measure the projection images from the target, which was rotated in



steps of  $90^\circ$  to obtain a set of four images over the  $0^\circ$ – $360^\circ$  angular range. For a DSSD thickness of  $500\ \mu\text{m}$ , the DSSD is considered to be suitable for charged particles and hard X-ray measurement at energies lower than 60 keV. Therefore, even though the  $\mu\text{C}-K_\alpha$  line from the sample with an energy of 75 keV could not be observed because of the low interaction efficiency with the DSSD, a peak with a mean value of 14.0 keV in the energy spectrum was clearly measured and identified as  $\mu\text{C}-L_\alpha$  from the sample. The projection images of the target at the four rotation angles reveal that the shape of Sample-1 and the rotation motion are in good agreement with the theoretical results. This demonstrates the potential of nondestructive elemental imaging method combined with the DSSD using muonic atoms. The further improvement of the imaging capabilities of the DSSD for a smaller sample will be possible using a new design for the imaging system, which will be more efficient for data acquisition. It is envisaged that imaging techniques using muonic X-ray measurements will be further developed in the future.

#### ACKNOWLEDGMENT

This research was partially supported by the Grant-in-Aid for Scientific Research on Innovative Areas (JP18H05457, B01 team of “Toward new frontiers: Encounter and synergy of state-of-the-art astronomical detectors and exotic quantum beams”). The muon experiment at the Materials and Life Science Experimental Facility of the J-PARC was conducted under the proposal of No.2019MS01.

#### REFERENCES

- [1] Terada, K., Ninomiya, K., Osawa, T. et al. *A new X-ray fluorescence spectroscopy for extraterrestrial materials using a muon beam* Sci Rep 4, 5072 (2014).
- [2] Terada, K., Sato, A., Ninomiya, K. et al. *Non-destructive elemental analysis of a carbonaceous chondrite with direct current Muon beam at MuSIC* Sci Rep 7, 15478 (2017).
- [3] Shimada-Takaura, K., Ninomiya, K., Sato, A. et al. *A novel challenge of nondestructive analysis on OGATA Koan's sealed medicine by muonic X-ray analysis* J Nat Med 75, 532–539 (2021).
- [4] Ninomiya, K., Kubo, M., Nagatomo, T. et al. *Nondestructive Elemental Depth-Profiling Analysis by Muonic X-ray Measurement* Analytical Chemistry 87, 4597–4600 (2015).
- [5] Hampshire, B.V., Butcher, K., Ishida, K. et al. *Using Negative Muons as a Probe for Depth Profiling Silver Roman Coinage* Heritage, 2, 400–407 (2019).
- [6] Kudo, T., Ninomiya, K., Strasser, P. et al. *Development of a non-destructive isotopic analysis method by gamma-ray emission measurement after negative muon irradiation*, Radioanal Nucl Chem 322, 1299–1303 (2019).
- [7] Takeda, S., Watanabe, S., Tanaka, S. et al. *Development of double-sided silicon strip detectors (DSSD) for a Compton telescope* Nucl. Instrum. Methods Phys Res A 579, 859–865 (2007).
- [8] Nakazawa, K., Takeda, S., Tanaka, T. et al. *A high-energy resolution 4 cm-wide double-sided silicon strip detector* Nucl. Instrum. Methods Phys Res A 573, 44–47 (2007).
- [9] Sato, G., Hagino, K., Watanabe, S. et al. *The Si/CdTe semiconductor camera of the ASTRO-H Hard X-ray Imager (HXI)* Nucl. Instrum. Methods Phys Res A 831, 235–241 (2016).
- [10] Watanabe, S., Tajima, H., Fukazawa, Y. et al. *The Si/CdTe semiconductor Compton camera of the ASTRO-H Soft Gamma-ray Detector (SGD)* Nucl. Instrum. Methods Phys Res A 765, 192–201 (2014).
- [11] Tajima, H., Nakamoto, T., Tanaka, T. et al. *Performance of a low noise front - end ASIC for Si / CdTe detectors in Compton gamma-ray telescope* IEEE Trans Nucl Sci 51, 842–847 (2004).
- [12] Takeda, S., Takahashi, T., Watanabe, S. et al. *Double-sided silicon strip detector for X-ray imaging* Spie Newsroom 01 (2008).
- [13] Wataru, H., Ryosuke, K., Naritoshi, K. et al. *Materials and Life Science Experimental Facility at the Japan Proton Accelerator Research Complex IV: The Muon Facility* Quantum Beam Sci 1, 11 (2017).
- [14] Agostinelli, S., Allison, J., Amako, K. et al. *Geant4—a simulation toolkit* Detect Assoc Equip 506, 250–303 (2003).
- [15] Jenkins, D. A., Kunselman, R., *Higher Transitions in  $\pi$ -Mesonic Atoms* Phys Rev Lett 17, 1148–1152 (1966).
- [16] Engfer, R., Schneuwly, H., Vuilleumier, J. et al. *Charge-distribution parameters, isotope shifts, isomer shifts, and magnetic hyperfine constants from muonic atoms* At Data Nucl Data Tables 14, 509–97 (1974).
- [17] Brownell, G.L. *Theory of radioisotope scanning* Intern J Appl Rad Isot 3, 181–192 (1958).